IEEE Access
Multidisciplinary | Rapid Review | Open Access Journal

Received July 3, 2020, accepted July 15, 2020, date of publication July 17, 2020, date of current version July 29, 2020.

*Digital Object Identifier 10.1109/ACCESS.2020.3010212*

# A Review for Solar Panel Fire Accident Prevention in Large-Scale PV Applications

**ZUYU WU[1], YIHUA HU[1,2], (Senior Member, IEEE), JENNIFER X. WEN[3], FUBAO ZHOU[4], AND XIANMING YE[5]**

[1]Department of Electronics Engineering, University of York, York YO10 5DD, U.K.
[2]Department of Electrical Engineering, China University of Mining and Technology, Xuzhou 221008, China
[3]School of Engineering, University of Warwick, Coventry CV4 7AL, U.K.
[4]Jiangsu Key Laboratory of Fire Safety in Urban Underground Space, China University of Mining and Technology, Xuzhou 221116, China
[5]Department of Electrical, Electronics, and Computer Engineering, University of Pretoria, Pretoria 0002, South Africa

Corresponding author: Yihua Hu (yihua.hu@york.ac.uk)

This work was supported by the U.K. Royal Academy of Engineering under Grant IAPP17/18.

**ABSTRACT** Due to the wide applications of solar photovoltaic (PV) technology, safe operation and maintenance of the installed solar panels become more critical as there are potential menaces such as hot spot effects and DC arcs, which may cause fire accidents to the solar panels. In order to minimize the risks of fire accidents in large scale applications of solar panels, this review focuses on the latest techniques for reducing hot spot effects and DC arcs. The risk mitigation solutions mainly focus on two aspects: structure reconfiguration and faulty diagnosis algorithm. The first is to reduce the hot spot effect by adjusting the space between two PV modules in a PV array or relocate some PV modules. The second is to detect the DC arc fault before it causes fire. There are three types of arc detection techniques, including physical analysis, neural network analysis, and wavelet detection analysis. Through these detection methods, the faulty PV cells can be found in a timely manner thereby reducing the risk of PV fire. Based on the review, some precautions to prevent solar panel related fire accidents in large-scale solar PV plants that are located adjacent to residential and commercial areas.

**INDEX TERMS** Photovoltaics, fire accident, solar panel, hot-spot effect, aging.

## I. INTRODUCTION

Solar photovoltaic (PV) panels have been widely applied to harness solar power for its renewable and environment-friendly features. However, the working environment of PV panels is usually not pleasant in practice, leading to fast aging and degradations of power generation, and even suffering from risks of fire accidents. According to [1], there is a 2% probability that a fire may occur to PV arrays each year with 0.6% of the fire accidents occurring in residential areas and 3.5% of them started from some rooftop PV modules.

When the solar panels catch a fire, it not only results in power generation reduction but also causes secondary damage such as toxic gas emission. As shown in Figure 1, the constituent materials of a PV panel are mostly organics. Energy released by glass fiber, ethylene-vinyl acetate and polyethylene terephthalate (PET) compounds in making epoxy resin printed circuit boards is 1.012, 0.54, 0.073 MJ, respectively based on the data from Tewarson and Quintiere [2]. Hydrogen compounds such as HF and HCL that are toxic are produced during the fire accident of solar panels. In 2009, 1826 PV modules with a generation capacity of 383 kW solar PV arrays were damaged in a fire accident in California, USA [3]. In the same year, another 15 events of solar PV module related fire accidents were reported in Netherlands [4]. In 2012, a solar panel related fire occurred in a warehouse in Goch, Germany, which caused a burning area of about 4000 $m^2$ [3].

The root cause of the solar panel related fire accident is usually associated with a deficit in the PV system. Previous analysis of solar panel fire events indicated that the causes of fire can be divided into two types, i.e. arc fault and spontaneous combustion [5], [6]. The main reasons of the arc failure include poor quality of PV modules, installation errors and DC arc ignition back board induced by junction and combiner boxes. Some aging solar panels, especially those with components not meeting their specified standards, can spontaneously ignite under high temperatures

The associate editor coordinating the review of this manuscript and approving it for publication was Lorenzo Ciani.

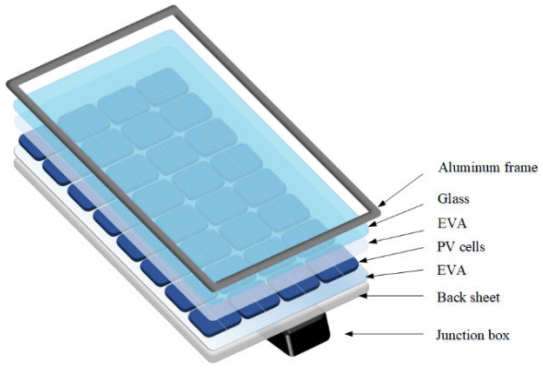


**FIGURE 1.** The structure of a PV module.

and sunlight due to chemical reactions and hot spot effects [7].

Solar panels can be made from crystalline silicon or amorphous. At present, the materials used for PV cells vary in different regions [8]. For example, according to Table 1, based on the characteristics of high melting point, low density, and good high-light performance, the crystalline silicon is suitable for the roof-top installation in residential areas. To avoid fire accidents, some fireproof obstacles must be installed between two modules, which effectively prevent the spread of fire in a large-scale PV array. Practically, more thin-film PV modules are used in urban areas. This, along with other technologies such as highly efficient CdTe single-junction cells can achieve the fastest response speed in the visible range. For example, based on the mean spectral ratio, which is the ratio of smoky and clear irradiance in Table 1, the value of CdTe is smaller than other PV cells. It is illustrated that the effect of smoke on CdTe is the greatest. Meanwhile, smoke in the near-infrared and infrared ranges has the least effect of monocrystalline silicon cells in visible range. It has the highest response due to the thin-film technologies (e.g., copper indium gallium selenide (CIGS) solar cells). These results have an impact on PV fire-prone areas [9], [10]. As for the protection from fire of ground PV array for commercial use, the installation distance between each module can be calculated according to different PV modules materials.

**TABLE 1.** Property of PV cells [10].

| | Monocrystalline | Polycrystalline | CdTe | GIGS |
|---|---|---|---|---|
| *Melting point* | 1420 °C | 1410 °C | 1092 °C | 986 °C |
| *Material density* | 2.32 g/cm$^3$ | 2.32 g/cm$^3$ | 5.85 g/cm$^3$ | 5.75 g/cm$^3$ |
| *Mean spectral ratio (smoky/clean)* | 0.9246 | 0.9211 | 0.9175 | 0.9213 |

In the large-scale PV arrays, the power generation mismatch accelerates the aging process of the solar panels [11] due to non-uniform patterns of shading, irradiance, and temperature of each panel. According to [12], approximately 51% of the PV related fire accidents is related to installation errors or poor quality of PV modules, which further causes cable faults on PV modules. On the contrary, the hot-spot effect is liable for a relatively lower percentage of the solar panel fire accidents. Low manufacturing quality of solar panels is a major contributor to the solar panel fire accidents. In order to reduce the risks of field solar panels related fire accidents, this review summarizes the cause factors and some effective fire prevention solutions to the field solar panels. There are two main solutions to alleviate the hot spot effect in PV arrays, namely restructuring PV modules and reconstruction of the distribution of PV arrays. As aged PV modules are easier to cause DC arc shock and damage, real-time fault detection mechanisms are helpful for preventing such damages. In addition, solar panels must be tested against strict engineering standards to reduce the risks of fire damage post installation.

In the following sections, a comprehensive review will be provided for solar panel fire accidents in large-scale PV applications. Section II illustrates the reasons of the solar PV related fire accidents, which include hot-spot effect, DC arc, and other conditions. In Section III, the methods for reducing the probability of the solar PV related fire accidents are discussed, which include structure reconfiguration and fault diagnosis. Section IV presents the conclusion.

## II. ROOT CAUSE ANALYSIS FOR SOLAR PANEL FIRE ACCIDENTS

According to the summaries of [2], [5]–[7], [12], [14]–[33], the main causes of PV fires are shown in Figure 2. There are 36% fire events due to installation errors, 15% accidents because of quality of PV modules [12]. Most fire events were found to be caused by DC arc [18]–[27] due to poor quality of PV modules, lack of drainage of PV systems, aging of combiner box, and aging of IGBTs in inverters. In addition, the hot spot effect should not be overlooked [14]–[17].

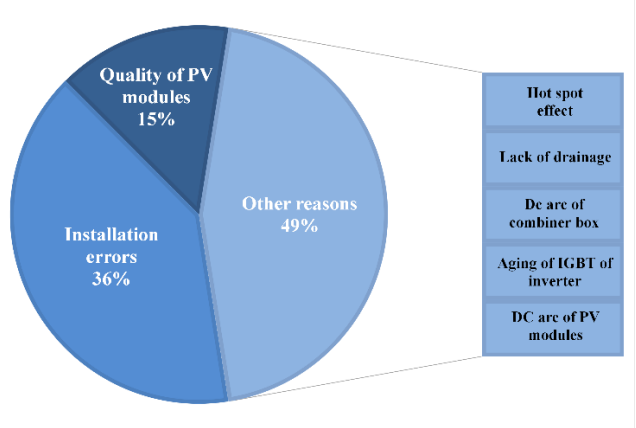


**FIGURE 2.** Factors lead to PV module fire accidents.

### A. THE HOT-SPOT EFFECT

In PV modules, series connected cells are usually used. Some PV cells suffer from partial shades from surrounding objects, such as fallen leaves, dust accumulation, and bird drops while other PV modules do not, hot spots may be produced due to non-uniform power generation status amongst the PV cells. The hot spot effect occurs if the temperature exceeds 5% above the standard temperature in a period in the standard testing condition (STC, 1000 W/m$^2$, 25 °C). Since the performance of PV cells is different in several cases, some shaded PV cells have obvious defects. The hot spot effect increases the local currents and voltages of PV modules, which results in a local temperature rise on the PV module, causing the modules to spontaneously ignite. Figure 3 shows a PV fire accident, which was caused by the hot spot effect.

**FIGURE 3.** Hot spot effect [13].

Under the STC condition, hot spot temperature of opaque PV modules is higher than that of semitransparent PV modules by 2–3°C, which drops with an increment as far as the numbers and areas of hot spots are concerned. Moreover, the efficiencies of PV modules have been predicted in the one and two hot-spot situations. For one-hot-spot situation, the efficiencies of opaque and semitransparent PV modules are 10.41% and 10.62%, respectively. In the two incidents involving hot spots, the efficiencies of the opaque and semitransparent PV modules are 10.41% and 10.54%, respectively [14]. Hu *et al.* [15] compared different degrees of shading and found that the minor size shading would cause the temperature of the PV panel in the shaded part to rise rapidly to cause a fire. Hu *et al.* [16] tried to conditions to obtain the condition of hot spot effect comparing different shading conditions on PV modules. They found that different levels of impacts result from different environments. The experimental conditions of the irradiance and surface temperature of PV panels are (820 W/m$^2$, 25 °C), (740 W/m$^2$, 22 °C), and (690 W/m$^2$, 24 °C), respectively. The shading comparison diagram is shown in Figure 4. For the first shading tests, three PV panels were connected in series with one of them covered with an opaque material to simulate the partial shades. It was recorded by the thermal imager that a hot spot was observed at the location of the shade. During the period of minor shading, the I-V curve was shifted dramatically. In Figure 4, $V_{m'}$ is the voltage of an unhealthy module, and $V_{array}$ is the voltage of the PV array. Figure 4 (b) shows the second shading test, where a PV module was partially covered by tissue paper to create a partial shade on the solar panel

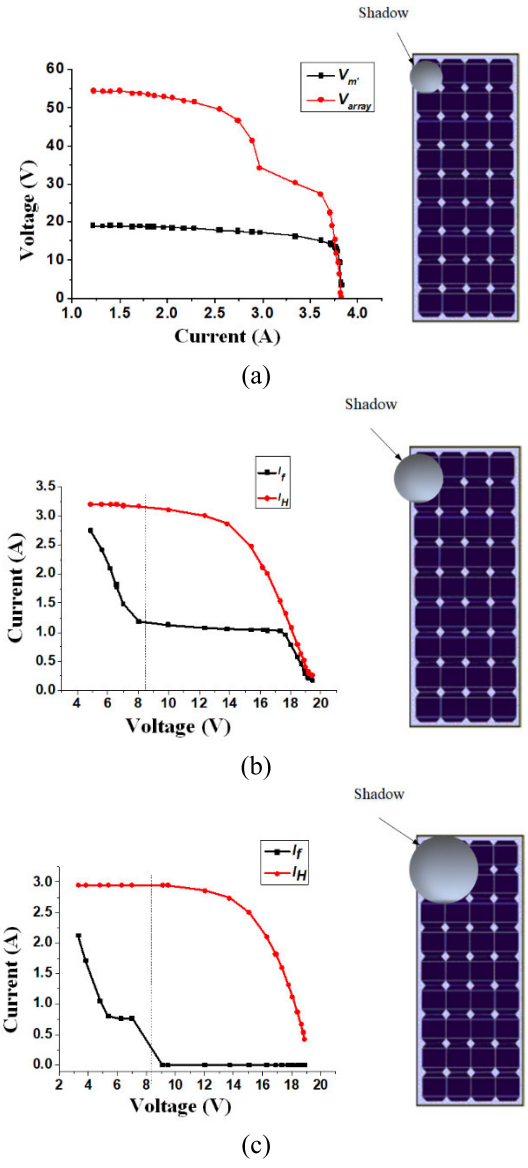


**FIGURE 4.** The types of PV shading. (a) 1st shading test (b) 2nd shading test (c) 3rd shading test [16].

so that certain lighting can penetrate the paper and reach the solar panel. In the experiment, the faulty power unit was short-circuited by a bypass diode when it cannot generate enough current to support the load, shown as the shift in the I-V curve. Where $I_f$ is the shaded module current, and $I_H$ is the healthy module current. As for the third shading test shown in Figure 4 (c), three PV panels were covered to create a large size of shade. In this case, the shaded PV areas were short-circuited through the bypass diode and all solar energy was converted into heat, such as the shift of $I_f$ in the I-V curve. However, a healthy PV panel can still convert the partial incoming solar energy into electricity, thereby decreasing the panel temperature. The comparative results shown in Table 2 illustrates that the only significant temperature increase is presented for the case with minor shading, which was prone to generate hot spots in PV modules.

**TABLE 2. Surface temperature of PV panels.**

| | 1st Test (820 W/m$^2$, 25°C) | 2nd Test (740 W/m$^2$, 22°C) | 3rd Test (690 W/m$^2$, 24°C) |
|---|---|---|---|
| *Unhealthy panel temperature* | 87.2°C | 33.8°C | 36.0°C |
| *Healthy panel temperature* | 44.3°C | 31.7°C | 33.7°C |

Simultaneously, Vasko *et al.* [17] observed the hot spots situations on PV cells, which were forward biased by a current power supply. After 30 mins heating, the temperature layer became non-uniform, and the hot spots were usually generated adjacent to bus bars. When the forward current of a PV cell exceeds a certain threshold, hot spots will occur under the forward bias conditions. The forward current is higher than the short circuit current in a healthy module because the short circuit current determines the upper limit of the module size before the hot spot formation becomes prohibitive. At the beginning of the electrical and temperature measurements, the voltage on the power supply was slightly different. Besides the formation of hot spots, the low temperature transient also caused by the initial heating and capacitive processes. With the hot spots appearance, the PV output voltage remained virtually the same, and the voltage and temperature of hot spot were linearly interrelated. Assuming that all the healthy PV modules in a PV array have the identical parameters concerning effective solar illumination intensity $S$ (kW/m$^2$), ambient temperature $T_a$ (°C) and total heat exchange coefficient $U_{pv}$ (W/m$^2$ · K). Fault diagnosis could be achieved based on Eq. (3), which is derived by (1) and (2). When the module faces a fault, the calculated $U_{pv}$ will be different from that of a healthy module [15].

$$S = V \cdot I + U_{pv} A_m (T_m - T_a) \tag{1}$$

$$T_a = \frac{[\frac{I_{mpp} V_{mpp}}{\eta_e - \mu(T_m - T_{ref})} - I_f \cdot V_f)]T_H - [\frac{I_{mpp} V_{mpp}}{\eta_e - \mu(T_m - T_{ref})} - I_{mpp} V_{mpp}]T'_H}{I_{mpp} V_{mpp} - I_f \cdot V_f} \tag{2}$$

$$U_{pv} = \frac{S - E}{A_m (T_m - T_a)} \tag{3}$$

where $T_m$ is the PV module temperature (°C); $T_H$ is the healthy PV module temperature (°C); $T_{H'}$ is the faulty PV module temperature (°C); $A_m$ is the PV module area (m$^2$); $E$ presents the electrical output power of the PV module (W); $I_f$ is the current of the healthy module in fault string (A); $V_f$ is the voltage of the healthy module in fault string (V); $T_{ref}$ is the reference temperature 25 °C; $V_{mpp}$ and $I_{mpp}$ are the voltage (V) and current (A) reached at the maximum power point, respectively. $\eta_e$ is the efficiency of the PV module at a $T_m$. For a silicon PV module, the efficient temperature coefficient is $\mu = 0.05\%/°C$.

In general, aging is accelerated if the PV panel is overheat over a long time. In addition, studies in [16] and [18] showed that when the solar irradiance is greater than 800W/m$^2$, the temperature difference between the maximum temperature of the hot spot and the average temperature of the module is about 10 °C. If fewer than 5% modules have a temperature difference of more than 10 °C, the PV array's power output remains stable. Therefore, even if there are partial shades and PV cell performance defects, the overheating part of the PV cell is not the load necessarily, and the hot spot effect may not occur. Even a hot spot effect occurs, its severity is also related to multiple factors. Since the hot spot effect is caused by a short-circuited PV cell, the current of the PV string produces a reverse bias. To avoid excessive reverse bias, current crystalline silicon components generally have two or three diodes in parallel to prevent hot spots in PV cells.

### B. CABLES AGING EFFECT

The arc is the phenomenon of glow discharge produced by the inter electrode electromotive force breakdown medium. Circuit and device damages are both likely to cause an arc failure. Once a DC arc occurs, PV panels will have a high probability to burn. As is shown in Figure 5, the arc failures of the PV system are divided into three kinds: series arc fault, parallel arc fault, and ground arc fault [18]. The series arc occurs mainly due to loose device interfaces, resulting in a small spacing, and current breakdown spacing. The parallel arcs usually occur between phase and neutral lines, as well as between phase lines because of broken line insulation. The ground arc refers to arc current flowing from a live conductor into the earth, which is usually caused by the failure of insulation in the high-voltage phase line.

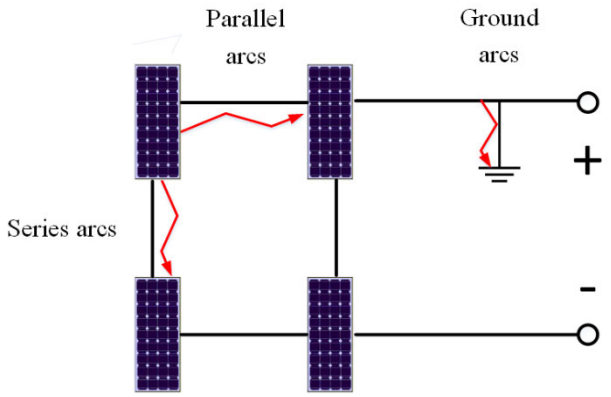


**FIGURE 5. Three types of PV arc failures.**

Some researchers have observed the significant damages of PV panel fire accidents through experiments and proposed the corresponding protection methods to prevent such accidents. Liao *et al.* [2] compared the four burning conditions of single-sided PV panels with the irradiance of 15, 20, 30, and 40 kW/m$^2$, respectively. The experiment setup is

shown in Figure 6. A high-power bulb is used as a predicted source to illuminate the front of the PV panel A, and at this time the natural combustion scenario of the PV panel is simulated. Then, PV panel B is ignited, and the heat transfer phenomenon of the adjacent PV panel is simulated. Finally, make the back of the C PV panel face up, simulating the scenario that the PV panel is ignited by the flame underneath it, when an arc fault fire accident occurs. According to the experimental results, at 15 kW/m$^2$ irradiance, the solar panel was on fire in 200s, but at 40 kW/m$^2$ irradiance, the solar panel was on fire in 25s. The PV panel is prone to fire accident when the irradiance exceeds 26 kW/m$^2$. This is a critical environmental condition as it takes shorter than 50s to cause a fire accident [19]. In [20], [21], when setting 10∼80 kW/m$^2$ of applied radiation intensity to simulate firing the flame radiant heat flow, the heat flux on the surface of the sample can be up to 70 kW/m$^2$ [22]. In the pre-experiment, it was found that the radiant heat flow of 30∼40 kW/m$^2$ can ignite the sample and be safe and controllable. Theoretically, the waste produced after a completely combustion of PV panels are carbon dioxide and water. However, because PET decays during combustion, its chemical bonds will be randomly reorganized. The carbon group of the PET molecular chain on the oxygen atom first attracts the hydrogen atom, and then the ester bond is broken down into acids and vinyl esters transitioned through the six-member rings state, and these cracked products are formed after some secondary processes [2]. Therefore, the decomposition products of PET combustion include CO, $CO_2$, acetaldehyde, aromatic acids, and vinyl esters. Besides, the outdoor oxidation is the most significant problem of ethylene-vinyl acetate film, which is caused by ultraviolet rays and humid hot $O_2$. Therefore, HF, HCL, $SO_2$, HCN and other flammable and toxic gases are generated after the final reaction. Among them, the hydrogen produced by HF or HCL causes secondary damages to PV panels.

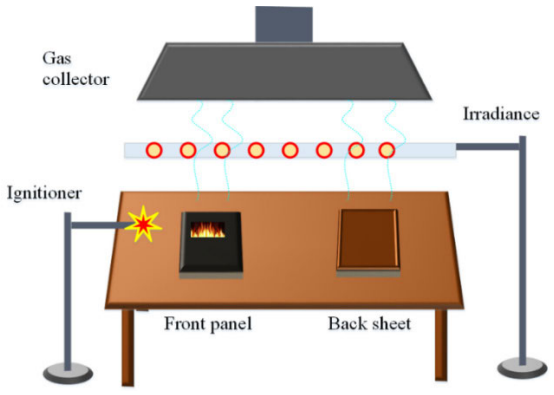


**FIGURE 6.** Experimental setup to simulate a fire accident of solar panels.

The relationship between the time of the fire and the radiation heat flow was obtained, which is $t^{-0.5} \propto q_e^n$ as shown in (4) [23]. Besides, the fire caused by the arc fault from TPT, which is the membrane of backboard of a PV module. The fire starts rapidly and becomes more intense from the membrane.

$$\frac{1}{\sqrt{t}} = \frac{1}{\sqrt{\pi}} \frac{2q_e^n}{\sqrt{k\rho c(T - T_0)}} \tag{4}$$

where $t$ is the ignition time (s), $q_e^n$ is the heat flux (W/m$^2$), $k$ is thermal diffusivity (W/m·K), $\rho$ is the air density (kg/m$^3$), $c$ is specific heat capacity (J/kg·K), $T$ is the thermal degree (°C) and $T_0$ is the reference thermal degree (°C).

Moreover, the increase in resistance of the components, heating, or arcing causes the components to burn out, which causes a fire. If any of the joints is loose, it may cause a DC arc, and consequently causes a fire [24], [25]. If the connector is not wrapped and protected properly to prevent infiltration of sand and dust, contact resistance of the connector will increase. When the ground wire is not connected, the equipment such as the combiner box lacks effective ground protection. Once there is a virtual connection or a lightning strike, it will cause a short circuit to ground, which not only degrades the power generation efficiency but also causes serious consequences such as a burning of the combiner box. As shown in Figure 7, explosion accidents during the combustion period in PV arrays have a large impact on the safety of operation and maintenance personnel. The explosion mainly come from the IGBTs and capacitors inside the inverter [26]. The power of a capacitor explosion can penetrate a 2 mm thick steel plate. The possible reasons for the destruction of the combiner box and DC cabinet include unreliable grounding, low cable insulation resistance, bad connector contact, or the wiring disorders, etc. [27].

**FIGURE 7.** Damaged combiner box by fire [28].

### C. OTHER CONDITIONS

PV modules may also suffering from physical damages. For instance, the cracks of PV modules are caused by the stress or pressure. If the welding area of the module is too small, it will easily cause the panel to rupture over a long time. Cracking is the main cause of fault of PV modules. These cracks are usually not visible to naked eyes and can only be detected through specific testing methods. All PV modules must have certain degrees of pressure resistance to prevent from being crushed. The quality of material (the choice of glass) and the manufacturing process are the main determinants of the PV module quality. The main reasons for the solar panel breakage are environment conditions, construction and installation method.

The low vacuuming temperature and foreign matter that enter the crack will generate bubbles, which will affect delamination and seriously cause the module to be completely scrapped, as shown in Figure 8. Component delamination is a serious problem because it allows moisture to penetrate, which will lead to catastrophic failure. At this point, the broken components on the panel need to be replaced. When moisture penetrates the protective layer of the solar module and contacts within the internal circuit, it seriously accelerates the degradation process of a PV module, which eventually leads to catastrophic consequences for the module and the entire PV system [29]. Gluing is caused by poor quality products and materials. Over time, the backplane sometimes turns yellow or brown. This is a chemical reaction between the inferior materials and sunlight. Once it begins to change color, ethylene-vinyl acetate will continue to change from its original state, inevitably causing damage to the material [30].

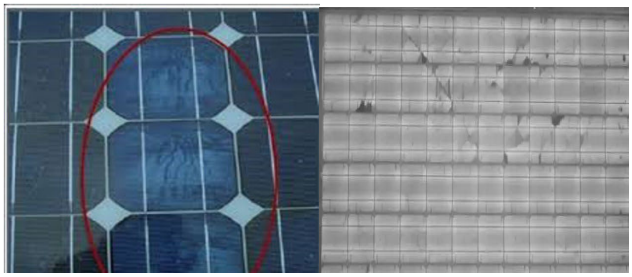

**FIGURE 8.** PV module crack [32].

Without good drainage measures on the roof-top, it is easy to cause water accumulation throughout the year. It not only leads to a decrease in PV efficiency, but also cause the aging and corrosion of cables, which may lead to fire accidents. For a ground PV array, the impact of rainwater may cause soil erosion, landslides, etc., so that the PV panels are seriously damaged [31].

Quality of Solar panels must be guaranteed by proper regulations. PV modules have to pass the test of UL 61730-2 "PV Module Safety Assessment Part 2: Test Requirements" [33], with a fire rating of C (basic fire proof rating). The components installed on buildings should at least reach the rating of C, and the price of PV modules with different fire proof ratings varies significantly. Components installed on existing roofs should be subjected to barrier tests and flame spread tests. Components used for roofing materials should be subjected to other subsequent test materials specified in UL 790 "Standard for Standard Test Methods for Fire Tests of Roof Coverings" [34]. There is no international standard for the combustion performance testing methods and judgment rules of modules on different buildings. The industry standard JG/T 492-2016 "General Technical Requirements for Building Photovoltaic Modules" [35] stipulates that PV modules should meet the flammability rating requirements of building materials or building modules in alternative locations and meet the requirements of GB8624 "Combustion Performance" [36]. Relevant regulations

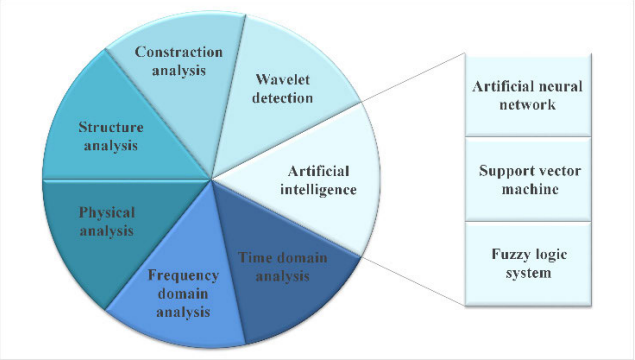


**FIGURE 9.** Detection methods for PV fires accidents.

on building materials, products, and their product classification, the fire resistance test methods and measurement rules need to comply with the provisions of GB15763.1 "Building Safety Glass Part 1: Fireproof Glass", GB/T 12513 "Fire-resistant test method for glass-encrusted components" and GB/T 9978.1 "Fire resistance test method of building components" [37]–[39].

To sum up, based on the above-mentioned PV production and installation standards, it can be found that the fire safety of PV-building integration is related the design of PV modules, and certification of the PV façade elements. The combination of good quality PV modules with a design-safe PV system can solve many of the safety issues observed so far.

## III. SOLUTIONS TO PREVENT PV FIRE ACCIDENTS

Depending on different fire-causing factors in the PV array, this section summarizes existing different solutions for different factors. Existing approaches to avoid solar PV fire accidents mainly include preventive actions. The preventive actions include array recombination and detection algorithm research. The studies [40]–[50] illustrate the reconfiguration of PV modules or PV arrays, and the studies [51]–[78] introduce algorithm to detect the faulty PV modules.

### *A. PREVENTIVE MAINTENANCE ACTION IN PV ARRAY*

In PV arrays, shades and dust accumulations are unavoidable, which are also the biggest threats to the safety of PV arrays. Therefore, some preventive maintenance actions such as conducting a periodical cleaning can be very effective in slowing the aging process of PV components and mitigating the hot spot effect.

#### 1) CONSTRUCTION ANALYSIS

There are currently two styles of solar panel installation: ground mounted and roof-top mounted. The surrounding environmental conditions, equipment conditions, and temperature changes of the project location need to be concerned for the ground mounted PV arrays [36]. Due to the influence of turbulent kinetic energy (TKE) among the modules, the soiling on the surface of the module must be uneven, resulting in the hot-spot effect and PV module fire accidents.

It is necessary to establish a flexible inspection and cleaning mechanism or use a data collection system to decide whether unplanned maintenance is necessary to reduce the risk of fire in different environments. However, if the distance between any two PV panels in the array is too far or too close, the PV array's generation capacity will be reduced. As shown Figure 10, the spacing $D$ between two PV panels should be large enough to avoiding shading effect, which is selected according to latitude, time angle, etc. The latitude angle ($\varphi$) of the winter solstice is ($-23.45$ °), and the time angle ($\omega$) corresponding to 9:00 am is 45 ° [41], [42]. In this case, not only the optimal photoelectric conversion efficiency can be guaranteed, but also the TKE value can be obtained to avoid the dust deposition. Therefore, calculating the distance between two panels according to (5) can obtain the most suitable distances between PV panels.

$$D = \cos A \bullet \frac{H}{\tan[\sin^{(-1)}(\sin\phi \sin\delta + \cos\phi \cos\delta \cos\omega)]} \tag{5}$$

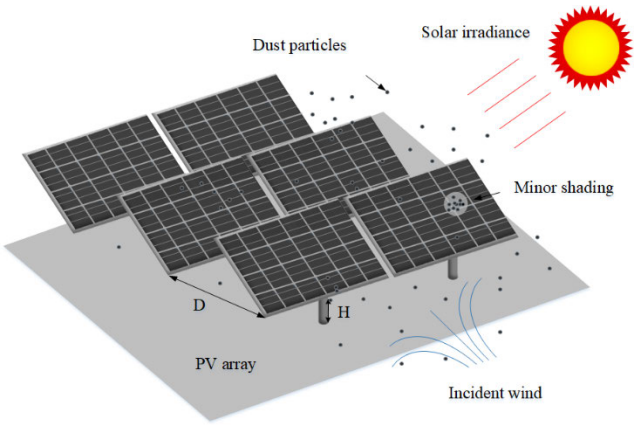


**FIGURE 10.** Dust deposition on a PV array.

where $D$ is the distance between obstacles (m), $A$ is the azimuth of the sun (°), $\varphi$ represents the latitude (°), $\delta$ means the declination (°), $\omega$ is the time angle (°) and $H$ is the PV array height difference (m).

Considering that the rooftop buildings are in close contact with people, the following factors need to be noted: 1) whether it can be avoided by string arrangement design or equipment technology improvement to personnel injured by the high voltage of the DC line in the event of a fire; 2) plan the location of the roof upper and lower channels and electrical equipment according to the meteorological data of the project location to reduce the time of power-off; Enough firefighting passages are provided to ensure rapid passage during a rescue. At the same time, the roof array distribution map is marked at the entrance of the bottom of the passage, and the opening and closing points of the power lines are marked. The marking should be easy to identify and well-marked to prevent fires. It can be cut off quickly; and 3) the module arrangement includes both horizontal and vertical arrangements, and the corresponding purlin arrangement also has two directions. When the module is arranged horizontally, the purlins are arranged vertically as shown in Figure 11. In this case, due to the chimney effect, the fire spreads faster than arrays with vertically arranged components [43]–[45].

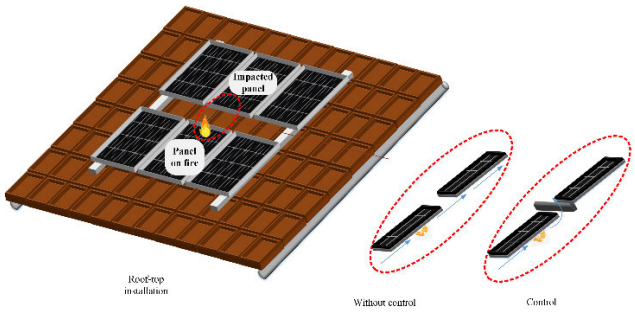


**FIGURE 11.** Solution to prevent PV fires on roof-top PV array.

Overall, strictly controlling the entry threshold of construction units, paying attention to environmental risks during the initial site selection, standardize cable connection construction, and establishing a reasonable operation and maintenance system and cycle according to the actual conditions of different projects can effectively reduce hidden dangers. By improving the technology and considering the design and training of the roof owner and local fire department, the impact of the fire can be reduced. That is to say, through comprehensive management before, during and after the accident, the loss can be minimized or avoided [46].

The impact of dust reduction on PV panels is enormous, both for the ground or rooftop mounted PV arrays. Formulas (6) is used to estimate dust flux around the PV array, and CFD simulation can accurately calculate the annual dust drop and dust distribution of a PV array, and thus can get a suitable cleaning cycle and cleaning method for the local PV array. Proper cleaning can effectively reduce the fire probability of PV arrays.

$$F_D = aEc\frac{\rho_\alpha}{g}u_*^3(1 + \frac{\frac{u_*}{\kappa}In(z/z_0)}{u_*})(1 - \frac{(\frac{u_*}{\kappa}In(z/z_0))^2}{u_*^2}) \tag{6}$$

where $E$ is the erosion factor, $\alpha$ is the sand blasting efficiency, $c$ is the empirical proportionality constant, $g$ is the gravitational acceleration (m/s$^2$), $\rho_\alpha$ is the air density (kg/m$^3$), $u_*$ is the friction velocity (m/s). $\kappa$ is a constant obtained empirically (about 0.35 for turbulent flow), and $z_0$ is the roughness length (m).

### 2) STRUCTURE ANALYSIS

Hot spots occur when the PV module is partially blocked, and part of the solar cell string becomes a reverse bias and dissipates energy in the form of heat. If the solar cell consumes more power than the maximum power of the PV cell, which maintain the maximum power under hot spot conditions, the PV cell will be completely damaged and open-circuit.

To protect the series PV cell, the bypass diodes are added on the PV cell string [47].

K. Kim proposed the first hot-spot mitigation technique that using bypass diodes to reconfigure PV modules [48]. The model structure is shown in Figure 12 (a). In the research, K. Kim shaded 1 of a 24-cell string, and found that a bypass diode imposes 0.5 V across the substring. However, there is still current passing through the shaded PV cell. Actually, the bypass diode can be treat as a load, which will not generate power. By using Kirchhoff's Voltage Law, the reverse voltage in the circuit can be describe in Eq. (7). Once hot spot is detected, there are two approaches to mitigate the potential risks. For short PV string (2∼3 cells), the traditional bypass diodes are more effective on reducing the probability of hot spots effect. For long PV string, a low reverse-breakdown PV cell limits the power dissipation in the hot spotting time. It is an effective prevention method if the power dissipation can be managed without damaging the cell.

$$V_R = (N-1)V_F + V_D \tag{7}$$

where $V_R$ is reverse voltage (V), $V_F$ is voltage drop (V), and $V_D$ is the diode voltage (V). *(N−1)* means the voltage drop from node 1 to node N.

The advantages of this technique is to reduce the temperature of solar cells in hot spots. Meanwhile, the probability of hot spots is also reduced for longer PV strings.

Based on the traditional bypass diode, S. Daliento proposed a modified bypass diode reconfiguration, namely, an ON-OFF MOSFET for PV modules in a hot-spot scenario [49], which is shown in Figure 12 (b). This method is applicable to any PV module, which composed of series connected cells. When the PV panel is partially shaded, this solution can significantly reduce the hot spot temperature by transferring the reverse voltage of the normal PV cells to the MOSFET of series connected in each sub-panel. To conclude, when the gate-source voltage ($V_{gs}$) is high, the MOSFET is short circuited. When $V_{gs}$ is low, there is a significant drain-source voltage drop $V_{DS}$ of MOSFET. The formula is shown below:

$$V_R = (N-1)V_F + V_D - V_{DS} \tag{8}$$

where $V_{DS}$ is the MOSFET drain–source voltage drop (V).

This method was verified by testing the reduction of hot spots temperature of polycrystalline silicon and monocrystalline silicon PV modules, which cooled down to about 20 °C and 24 °C, respectively.

Based on the single ON-OFF MOSFET switch circuit, M. Dhimish proposed a double MOSFET switch circuit, which is more effective to mitigate the hot spots effect [50]. The model is shown in Figure 12 (c). The switch 1 is connected in series with the PV cells, and the general state is ''on''. When hot spot situation is occurred, switch 1 will open to further alleviate the hot spot effect. The switch 2 is in parallel connection with the PV cells, and the general state is ''off''. When the PV string is open, it will open to circulate current. To ensure the health of the PV module, switch 2 is

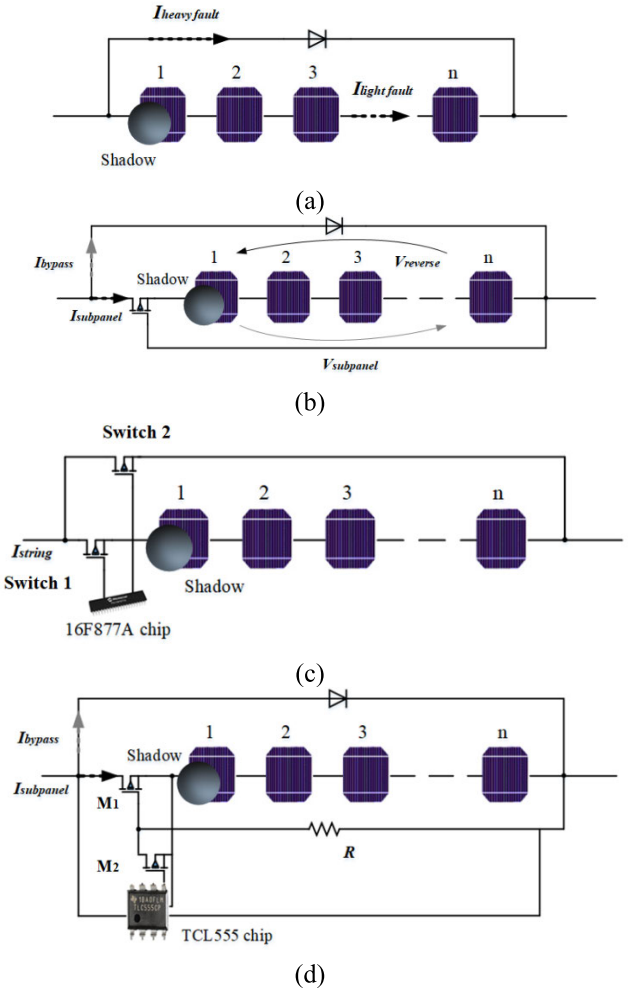


**FIGURE 12.** Reconfiguration of PV string. (a) bypass diode circuit (b) ON-OFF MOSFET circuit (c) 16F977A microcontroller circuit (d) TCL555 microcontroller circuit.

controlled by 16F877A microcontroller and activated twice every three hours. Because M. Dhimish found that three hours is the maximum allowable duration before the hot spot reappears in the PV cells, and the number of activations is determined by thermal image analysis. As for the 16F877A, it is a microcontroller-based system that prevents hot-spot operation using open-circuit PV modules. This method not only reduces the heat spot temperature by 17 °C, but also increases the output power by 3.8%.

Simultaneously, P. Guerriero proposed a new bypass diode circuit, which is an evolution circuit from S. Daliento [49]. The diagram is shown in Figure 12 (d) [51]. In the circuit, the drain-source voltage drop of MOSFET M1 supplies power to the TLC555 digital oscillator, and its output voltage drives MOSFET M2. Therefore, as long as M1 works normally, the oscillator is turned off, its output is low, and M2 is also turned off. When a part of the PV cells is blocked, the drain–source voltage drop of M1 increases, and the oscillator turns on and begins to provide an output signal that alternates between high and low. The output signal remains

high for approximately 97% of the time. During this time interval, M2 is on, so M1 remains off. Conversely, if there is no longer partial occlusion, M1 is turned on, its drain–source voltage drop is decreased, and the oscillator is turned off, returning to normal operating conditions.

This method can reduce the hot spot temperature to 50 °C and increase the output power by 8% in a shadow-shaded scenario. Different from others, this solution address the rising in temperature of shaded cells completely. Meanwhile, the oscillator will not generates more power on bypass events, due to the oscillator is sleeping in the rest time.

By changing the structure of the PV string, as well as by some controllers, the probability of hot-spot effect can be effectively reduced. This method not only reduces the risk of a PV array, but also increases the power of PV output [52].

### B. FAULT DIAGNOSIS

In 2011, the U.S. Insurer Laboratory (UL) launched UL Standard 1699B draft [53], which is the DC arc detection standard of circuit safety outline of DC arc fault protection for the PV systems [54]. At present, numerous methods could detect the arc fault of PV systems: physical analysis (clustering method) [55]–[58], Fast Fourier Transform (frequency domain analysis) [59]–[63], time domain analysis [64]–[67], wavelet detection (multi-resolution analysis) [68]–[77], and Artificial Intelligence method (neural networks, support vector machines, fuzzy logic systems, etc.) [78]–[86].

#### 1) PHYSICAL ANALYSIS

In the event of an arc failure, the heat, arc, noise, or electromagnetic signals will be emitted. The physical analysis is based on the physical properties of sound, light, and radiation are detected by cluster method. As for the famous and widely use physic-based model, Myer arc model is suitable for low current arcs [55], which assumes that thermal causes power loss, and the formula is shown below:

$$\frac{1}{g}\frac{dg}{dt} = \frac{1}{\tau}\left(\frac{i_{arc}^2}{P} - 1\right) \tag{9}$$

where $g$ is arc conductance (S), $i_{arc}$ is arc current (A), $P$ is the static cooling power (W), and $\tau$ is the arc time constant determined empirically (s).

In addition, Peng *et al.* used fuzzy logic to indicate clustering to detect arc failure [56]. The mold maximum value of the electromagnetic radiation signal of the fault arc after noise reduction is selected as the fault criterion. In [57], the Hilbert antenna is used to measure the electromagnetic radiation signal of the DC arc, the frequency of the electromagnetic radiation signal, the pulse interval, and the pulse cluster duration as the basis for the failure. Physical-based detection methods install devices in local locations in the system, making it easier to locate fault locations [58]. However, because these models involve many parameters, the operation is complex and is not easy to be implemented.

#### 2) FAST FOURIER TRANSFORM

Fourier Transform is a classical frequency domain-based method, and it is recommended to carry out fault detection in the frequency band of 1 to 100 kHz [59], [60]. The time of the Fast Fourier Transform (FFT) detection method is less than 16 ms. It effectively disconnects the arc from the inverter in the DC micro grid. While, this algorithm may not effective at the converter startup. In this case, the time domain changes dramatically and the size of the high-frequency content in the frequency domain increases like an arc failure leading to unnecessary tripping [61], [62].

The FFT transformation of single current mutation and electromagnetic radiation waveform is carried out and its spectral characteristics are analyzed. The spectral characteristics of current and electromagnetic radiation signals are similar, with the largest frequencies as 13MHz. The electromagnetic radiation field is proportional to the current rise rate, at the beginning of the current steep rise edge, the inductor of the arc is close to 0. Estimated maximum amplitude of arc electromagnetic radiation spectrum is based on (10) [63]:

$$f_0 = \frac{1}{2\pi\rho\varepsilon} \tag{10}$$

where $\varepsilon$ is the dielectric constant of the air (F/m), and $\rho$ is the arc resistivity (kg/m$^3$).

According to (8), the frequency with the largest amplitude in the electromagnetic radiation spectrum is only related to the arc resistance and the dielectric constant in the air. The resistivity of arcs generated by different inter-polar distances and electrode diameters may vary, and the frequency of electromagnetic radiation in DC arcs may be different. Therefore, the pulse interval, characteristic frequency, and duration of the arc electromagnetic radiation signal can detect DC arc failure as feature parameters.

#### 3) TIME DOMAIN ANALYSIS

The advantage of time domain analysis is intuitive and accurate. The time domain representation of the system output can be obtained from differential equations or transfer functions. In [64], [65], the accuracy rate of fault detection in a PV module detected by Minimum Covariance Determinant (MCD) estimator under STC is 98%, and the false alarm rate is 0.01%. This method is to operate the voltage and current of different PV modules into the MCD estimator at the same time instant. Then, the distribution of the I-V curve to the centerline of each PV module can be used to detect arc faults. The MCD estimator can be determined as (11).

$$\alpha = \frac{med_i((x_i - \hat{\mu_S})^T \hat{C_S^1}(x_i - \hat{\mu_S}))}{m} \tag{11}$$

where $\hat{\mu_S}$ and $\hat{C_S}$are estimates of sample mean and covariance matrix computed using the MCD estimator, and $x_i$ is a data subset.

In [66], Schimpf *et al.* used Finite Impulse Response (FIR) estimator to detect the arc fault. The idea of this method is

that when the arc detector is integrated into the PV module, the detector can only measure and monitor the PV current and the PV voltage. Due to the need for shunt resistors, Hall sensors or current transformers, the only signal used as the arc detector input is the PV voltage. The arc voltages measured on the PV module various significantly according to their position in the system. The operation of FIR estimator fault detection is that first passing the input signal through a bandpass filter whose cut-off frequencies are 1 kHz and 7.5 kHz. The estimator then compares the current signal value to the previous value, and when the difference is 0, the system is fault-free.

In [67], Yao *et al.* found that the selection of time window length will impact the current waveform pattern. The research shows that time domain analysis, although simple, is very effective in identifying arc failures. Because it has long enough time to ensure the randomness of the test.

#### 4) WAVELET ANALYSIS

At present, wavelet analysis is the mainstream detection method, which is gradually multi-scale refinement of signal functions through telescopic translation operation, and finally reach the high frequency time segmentation, low frequency subdivision, so as to focus on any details of the signal [68]–[71]. According to the fault signal, it sets the motion threshold of the fault alarm device in normal state and in different value range, thus solving the difficult problem of Fourier transformation. Wu *et al.* [72] selected the db4 wavelet for wavelet decomposition, selected the energy value of the wavelet high-frequency component as the fault standard, and used the reliable value between the normal state and the fault state as the fault alarm threshold. Meanwhile, Lu *et al.* [73] selected the standard deviation as the characteristic in the time domain, took the energy of each band after the db5 wavelet decomposition as the frequency domain feature, constructed the feature plane, and divided the fault critical line within the feature plane to detect the arc. The maximum signal and wave detail are determined by experiments. The variance and model values of the numbers are the three time-frequency domain standards, and time domain-based measurements are proposed. Mix the condition with the arc fault of the frequency domain, and the judgment of this method has a single method with high precision and reliability, which further reduces the error rate and suppression rate of the detection method [74]. The accuracy of wavelet decomposition fault detection is 100% [67], [75].

According to the basic principle of time-domain emission method [76], the relative position of the fault point and the measuring point can be calculated as:

$$dis = \frac{v\tau}{2} \tag{12}$$

where $v$ is the wave speed in the cable (m/s); $\tau$ is the signal of time-delay value in the fault.

For a row wave, if the distance of propagation $L$ along the cable within a cycle time $T$, the propagation speed of the wave is $v$, then, it can be obtained that:

$$v = \frac{L}{T} \tag{13}$$

When the transmission line loss is very small or the test signal is high frequency, the wave speed can be derived as:

$$v = \frac{2\pi f}{\beta} = \frac{\omega}{\beta} = \frac{\omega}{\omega\sqrt{LC}} = \frac{1}{\sqrt{L_0 C_0}} \approx \frac{c}{\sqrt{\mu_r \varepsilon_r}} \tag{14}$$

where $c$ is the speed of light, which is $3 \times 10^8$ m/s; $\mu_r$ is the relative magnetic guide coefficient of the medium around the cable at high frequencies; $\varepsilon_r$ is the relative dielectric constant of the medium around the cable at high frequencies.

According to (14), the transmission speed of the pulse wave in the cable is not related to the structure, length, conductor material. It only depends on the relative magnetic conductivity and relative dielectric constant of the cable insulated medium. For cables made of different conductor materials, the insulation medium is the same and the signal travels at the same speed inside it.

This method fills the blank of arc fault detection and positioning on the DC bus in the PV system, and effectively prevents accidents caused by arc failure. Because the detection signal of this method has sharp self-correlation, it can have the good anti-jamming ability and high accuracy in the on-line detection and positioning of DC bus arc fault [77].

#### 5) ARTIFICIAL INTELLIGENCE METHOD

In recent years, artificial neural networks (ANN), support vector machines (SVM), fuzzy logic, and other intelligence algorithms have replaced thresholds to decide whether there is arc fault.

The ANN aims to obtain the model through learning, and use the model to predict the desired target value. In the field of arc detection, the position of DC arc can be detected by using the data of neural network. He *et al.* in [78] uses an RBF neural network to judge arc fault, but it is easy to local optimization and slow training. The study [79] uses a genetic algorithm optimized BP neural network to judge arc fault. The ANN method is fast and accurate for arc detection [80].

The arc detection neural network model is shown in Figure 13, uses a three-tier structure [81], where $P$ is the input matrix; $i$, $j$, and $k$ represent the number of nodes at each layer respectively; $w_{ij}$ is the weight between the implied layer $j$ node and the output layer $i$ node, and $w_{jk}$ is the weight between the node $k$ of the output layer and the node $j$ of the implied layer. The implied layer activation function selects the S-type activation function, and the output layer activation function selects the linear activation function.

(a) Input layer: Input layer nodes are related to the number of input data. The input to the model is the 12th to 31st harmonics after the FFT, so the junction of the input layer is 20.

(b) Implied layer: Implied layer nodes are not fixed and can be adjusted as needed. Currently, there is no universal way to determine the number of implied layer

**TABLE 3.** Fire proof solutions of pv modules.

| *Method* | Adopted technique | Advantage | Disadvantage | Accuracy | Reference |
|---|---|---|---|---|---|
| *Distance of each PV panel (ground mounted PV modules)* | Design the optimal spacing between each panel | Avoid the hot-spot effect while ensuring maximum power capacity of the PV array | Error in the amount of dust accumulation on the surface of PV panels | Not mention | [36][41-42] |
| *Obstacle of each PV panel (roof-top mounted PV modules)* | The baffle is used to block the air flow between each panel | Blocking the airflow between PV panels reduces the flame burn trend | Increased roof load, and the rescue of firefighters made it more difficult | Not mention | [43-46] |
| *Structure analysis* | Add bypass diode or MOSFET in the circuit | Reducing hot-spot effect and improve the power efficiency | Increased cost of PV modules | Not mention | [47-51] |
| *Physical analysis* | Detect arc faults through physical properties | High accuracy on small collections of data with less than 200 data objects | These models involve many parameters, the operation is complex and is not easy to implement in simulation | High | [55-58] |
| *Frequency domain analysis* | Detect arc faults by using FFT in the frequency domain | Fast and high universal | This algorithm may not work properly at the inverter or converter startup. It is easily to trip. | Below 90% | [80] |
| *Time domain analysis* | Detect arc faults through estimators in the time domain | Intuitive, high accuracy, and easy to operate | Constrained by time window | 98% | [64-65] |
| *Wavelet detection* | Detect the arc faults through the wavelet at time-frequency domain | Effective and directly | Limited by vibration diagnostic and analytical instruments, resolution, and analysis software functions. | 100% | [67][75] |
| *Artificial intelligence detection* | Detect the position of DC arc by using ANN, SVM, and fuzzy logic system. | High accuracy, easy, and convenient | Need a huge data-base | About 99% | [83-84] |

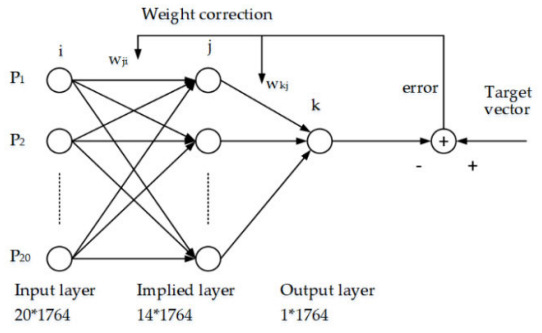


**FIGURE 13.** Arc detection neural network model [81].

nodes. If the number of nodes is too small, the network performance is poor or cannot be trained, if too much selection, although the error can be reduced, but will increase the network training time, easy to fall into the local minimum point and not reach the optimal solution. The determination of the number of implied layer nodes is obtained by the formula (15) [82].

(c) Output layer: The output layer only needs one node, the output with 0 and 1 respectively to represent the arc-free and arc-less.

$$n = \sqrt{n_1 + n_0} + \beta \tag{15}$$

where $n$ is the implied layer junction, $n_1$ is the input layer junction, $n_0$ is the output node, and $\beta$ is the constant between 1 and 10.

According to (16) and combined with the results of a large number of experiments, it is found that the training effect is best when the implied layer node points take 14.

In addition, the studies [83] and [84] use the SVM algorithm to extract the mean current and high-frequency components from the time-frequency domain. Fault criteria is

used to train the model, and the obtained model can classify whether an arc fault occurs.

SVM is a better supervised learning algorithm. This algorithm is used to solve the separation hyperplane problem that can divide the training data set normally and has a very large geometric interval. As shown in the Figure 14, all of the "circle" means training data, among them, the red circle is the support vector. "Wx+b=0" means the separation hyperplane. Actually, there are countless hyperplanes corresponding to linearly separable data sets. Among them, the separation hyperplane with the largest geometric interval is unique. Compared with ANN, SVM searches the global minimum data during training, while ANN will only search the local minimum data. And the performance of SVM is highly related to the quality of training data.

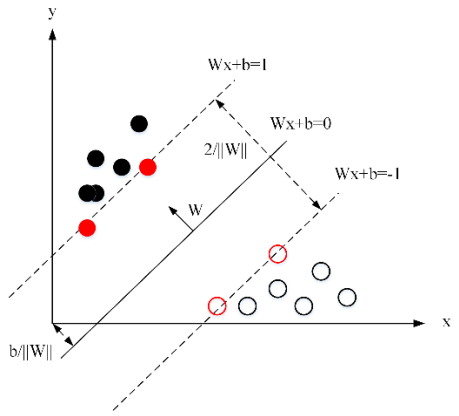


**FIGURE 14.** An diagram of SVM trained samples [74].

In [85] and [86], the authors used fuzzy logic system to detect the arc fault in the PV array. The accuracy of this method is increased up to 98.8%. The operation of the arc detection system based on fuzzy logic is: First, input the initial signal to the fuzzification process. Then, use predefined rules to classify arc faults and normal operation. It should be mentioned that the rules in fuzzy systems are designed based on the fault modes and mechanisms.

### C. DISCUSSION

The method of fire prevention and detection of PV Arrays can be summarized as the optimal distance method (ground mounted PV array), obstacle-adding method (roof-top mounted PV array), and reconfiguration of PV components, physical analysis, frequency domain analysis, time domain analysis, wavelet detection, and the artificial intelligence algorithm. The advantages and disadvantages of these methods are shown in Table 3. Due to the increasing fault cases, there are many data-base can be used in the future. Therefore, the artificial intelligence methods will be concerned popular in the future.

Based on these methods, the isolation device can be added to PV arrays with fireproof materials, and the alarm system can be set up according to the intelligent algorithm to identify the DC arc failure, thus minimizing the probability of a PV fire. In addition, the safety training of the firefighters is essential due to the large amount of toxic gases produced by PV combustion [87].

## IV. CONCLUSION

The safety of PV power generation and PV arrays is receiving increasing attention, especially the need to reduce the possibility of fire and timely maintenance. The hot spot effect and aging of PV panels were found responsible in previous fire accidents can be caused by the dust density around the PV array, the ambient temperature, and the material structure of the PV array. Preventive solutions to the fire accident can be distinguished into solar panel reconfiguration and fire fault detection algorithm. The advantages of reconfiguration of PV modules include reducing hot spot and improving power efficiency. Meanwhile, the advantage of the fire fault detection algorithm is to detect faulty position accurately.

In order to reduce the probability of PV fire accident, there are technical specifications to comply. Firstly, the PV module needs to pass the UL 790 "Safety Standard for Roofing Material Fire Test" combustion and flame spread test. Secondly, the inverter should be designed without fuses to avoid fire caused by DC side faults. The inverter internal transformer, PCB board and other internal components prone to high temperature should be made of non-combustible or non-combustible materials. Thirdly, the internal components of the junction box, control equipment, and power distribution equipment should be made of non-combustible materials. Fourthly, all cables are required flame retardant coating and made of low smoke, and low toxicity materials. Fifthly, fireproof sealing measures should be applied to holes, such as cable inlets and outlets of power distribution equipment in houses, equipment inlet holes, cable inlets and outlets of junction boxes, cable penetration holes, cable trenches, and cable trench interfaces.

In addition to research on the mechanism and prevention of PV fires, it is also necessary to consider fire safety issues of PV-building integration. In order to improve the safety of fire prevention and extinguishing of PV systems, it is basal to conduct fire risk investigation and hazard assessment. Test and evaluate the combustion properties and fire resistance of PV modules. Secondly, considering the impact on building safety, it is advised to conduct a comprehensive risk assessment for potential failure units of PV building integration. Design fire separation facilities and use fireproof materials to reduce losses caused by fire accidents. Thirdly, realize the management intelligentization of electrical fire monitoring and early warning, and strengthen the investigation of hidden fire hazards of the equipment. Specifically, the fire prevention and control system can automatically identify and eliminate fire risks. For example, set up an appropriate automatic fire alarm system, intelligent protection against DC arc, and intelligent blocking components. Finally, it is also critical to strengthen the daily fire supervision and management, and regularly hold the fire safety training on PV power generation.

## REFERENCES


[1] P. D. Moskowitz and V. M. Fthenakis, "Toxic materials released from photovoltaic modules during fires: Health risks," *Sol. Cells*, vol. 29, no. 1, pp. 63–71, Jun. 1990.

[2] B. Liao, L. Yang, X. Ju, Y. Peng, and Y. Gao, "Experimental study on burning and toxicity hazards of a PET laminated photovoltaic panel," *Sol. Energy Mater. Sol. Cells*, vol. 206, Mar. 2020, Art. no. 110295.

[3] J. Sipe, "Development of fire mitigation solutions for photovoltaic (PV) systems installed on building roofs," Fire Protection Res. Found., Denver, CO, USA, Tech. Rep., Jul. 2016, doi: 1600223.000-5873.

[4] (Feb. 20, 2013). *Business Counselor Office in The Netherlands. Dutch Solar Panel Accidents Occur Frequently*. [Online]. Available: http://www.mofcom.gov.cn/article/i/jyjl/m/201302/20130200032328.shtml

[5] G. Manzini, P. Gramazio, S. Guastella, C. Liciotti, and G. L. Baffoni, "The fire risk in photovoltaic installations–test protocols for fire behavior of PV modules," *Energy Procedia*, vol. 82, pp. 752–758, Dec. 2015.

[6] S. S. Nair, "A survey report of the firefighters on fire hazards of PV fire," in *Proc. IEEE Int. Conf. Syst., Comput., Automat. Netw. (ICSCA)*, Jul. 2018, pp. 1–5.

[7] J. H. Wohlgemuth and S. R. Kurtz, "How can we make PV modules safer?" in *Proc. 38th IEEE Photovoltaic Spec. Conf.*, Jun. 2012, pp. 003162–003165.

[8] C. Lamnatou, G. Notton, D. Chemisana, and C. Cristofari, "Storage systems for building-integrated photovoltaic (BIPV) and building-integrated photovoltaic/thermal (BIPVT) installations: Environmental profile and other aspects," *Sci. Total Environ.*, vol. 699, Jan. 2020, Art. no. 134269.

[9] M. Perry and A. Troccoli, "Impact of a fire burn on solar irradiance and PV power," *Sol. Energy*, vol. 114, pp. 167–173, Apr. 2015.

[10] G. N. Tiwari, R. K. Mishra, and S. C. Solanki, "Photovoltaic modules and their applications: A review on thermal modelling," *Appl. Energy*, vol. 88, no. 7, pp. 2287–2304, Jul. 2011.

[11] D. P. Winston, S. Kumaravel, B. Praveen Kumar, and S. Devakirubakaran, "Performance improvement of solar PV array topologies during various partial shading conditions," *Sol. Energy*, vol. 196, pp. 228–242, Jan. 2020.

[12] C. Coonick, "Fire and solar PV systems-investigations and evidence," breNational Solar Centre, Tech. Rep. P100874-1004, May 2018, no. 2.9.

[13] *Count the Three 'Pits' You Don't Know in the Photovoltaic System*. (in Chinese). Accessed: Nov. 4, 2016. [Online]. Available: https://www.china5e.com/m/news/news-229160-0.html

[14] P. Rajput, G. N. Tiwari, and O. S. Sastry, "Thermal modelling and experimental validation of hot spot in crystalline silicon photovoltaic modules for real outdoor condition," *Sol. Energy*, vol. 139, pp. 569–580, Dec. 2016.

[15] Y. Hu, W. Cao, J. Ma, S. J. Finney, and D. Li, "Identifying PV module mismatch faults by a thermography-based temperature distribution analysis," *IEEE Trans. Device Mater. Rel.*, vol. 14, no. 4, pp. 951–960, Dec. 2014, doi: 10.1109/TDMR.2014.2348195.

[16] Y. Hu, B. Gao, X. Song, G. Y. Tian, K. Li, and X. He, "Photovoltaic fault detection using a parameter based model," *Sol. Energy*, vol. 96, pp. 96–102, Oct. 2013.

[17] A. C. Vasko, A. Vijh, and V. G. Karpov, "Hot spots spontaneously emerging in thin film photovoltaics," *Sol. Energy*, vol. 108, pp. 264–273, Oct. 2014.

[18] N. L. Georgijevic, M. V. Jankovic, S. Srdic, and Z. Radakovic, "The detection of series arc fault in photovoltaic systems based on the arc current entropy," *IEEE Trans. Power Electron.*, vol. 31, no. 8, pp. 5917–5930, Aug. 2016, doi: 10.1109/TPEL.2015.2489759.

[19] B. Lecouvet, M. Sclavons, S. Bourbigot, and C. Bailly, "Thermal and flammability properties of polyethersulfone/halloysite nanocomposites prepared by melt compounding," *Polym. Degradation Stability*, vol. 98, no. 10, pp. 1993–2004, Oct. 2013.

[20] A. Ito and T. Kashiwagi, "Characterization of flame spread over PMMA using holographic interferometry sample orientation effects," *Combustion Flame*, vol. 71, no. 2, pp. 189–204, Feb. 1988.

[21] P. A. Beaulieu and N. A. Dembsey, "Effect of oxygen on flame heat flux in horizontal and vertical orientations," *Fire Saf. J.*, vol. 43, no. 6, pp. 410–428, Aug. 2008.

[22] M. B. Ayani, J. A. Esfahani, and R. Mehrabian, "Downward flame spread over PMMA sheets in quiescent air: Experimental and theoretical studies," *Fire Saf. J.*, vol. 41, no. 2, pp. 164–169, Mar. 2006.

[23] M. A. Delichatsios, "Piloted ignition times, critical heat fluxes and mass loss rates at reduced oxygen atmospheres," *Fire Saf. J.*, vol. 40, no. 3, pp. 197–212, Apr. 2005.

[24] M. C. Falvo and S. Capparella, "Safety issues in PV systems: Design choices for a secure fault detection and for preventing fire risk," *Case Stud. Fire Saf.*, vol. 3, pp. 1–16, May 2015.

[25] K. Murata, T. Yagiura, K. Takeda, M. Tanaka, and S. Kiyama, "New type of photovoltaic module integrated with roofing material (highly fire-resistant PV tile)," *Sol. Energy Mater. Sol. Cells*, vol. 75, nos. 3–4, pp. 647–653, Feb. 2003.

[26] K. Chen, C. Huang, and J. He, "Fault detection, classification and location for transmission lines and distribution systems: A review on the methods," *High Voltage*, vol. 1, no. 1, pp. 25–33, Apr. 2016, doi: 10.1049/hve.2016.0005.

[27] C. Luping, W. Peng, and X. Liangjun, "Novel detection method for DC series arc faults by using morphological filtering," *J. China Universities Posts Telecommun.*, vol. 22, no. 5, pp. 84–91, Oct. 2015.

[28] *How to Distinguish the Hot Spot Effect and PID Effect of Photovoltaic Modules*. (in Chinese). Accessed: Aug. 7, 2019. [Online]. Available: https://www.nengapp.com/news/detail/3043104

[29] S.-K. Lee, C.-M. Wu, and K.-C. Hung, "A study on fire risks to firefighters in the building with photovoltaic system," in *Proc. Int. Conf. Appl. Syst. Innov. (ICASI)*, May 2017, pp. 1174–1177.

[30] J. K. Hastings, M. A. Juds, C. J. Luebke, and B. Pahl, "A study of ignition time for materials exposed to DC arcing in PV systems," in *Proc. 37th IEEE Photovoltaic Spec. Conf.*, Seattle, WA, USA, Jun. 2011, pp. 003724–003729.

[31] R. Tommasini, E. Pons, F. Palamara, C. Turturici, and P. Colella, "Risk of electrocution during fire suppression activities involving photovoltaic systems," *Fire Saf. J.*, vol. 67, pp. 35–41, Jul. 2014.

[32] *Three Types of Problem Detection Methods for Photovoltaic Modules*. (in Chinese). Accessed: Dec. 1, 2017. [Online]. Available: https://kknews.cc/zh-my/news/bkg4xv6.html

[33] *PV Module Safety Assessment Part 2: Test Requirements*, Standard UL 61730-2, 2017.

[34] *Safety Standards for Roof Fire Tests*, Standard UL 790, 2018.

[35] *General Technical Requirements for Building Photovoltaic Modules*, Standard JG/T 492, 2016.

[36] *Combustion Performance*, Standard JG/T 492, 2006.

[37] Y. Zheng, "Analysis on fire safety of integrated photovoltaic building system," (in Chinese), *Fire Sci. Technol.*, vol. 38 no. 5, pp. 721–723, May 2019.

[38] L. Mazziotti, P. Cancelliere, G. Paduano, P. Setti, and S. Sassi, "Fire risk related to the use of PV systems in building facades," in *Proc. MATEC Web Conf.*, vol. 46, 2016, p. 05001, doi: 10.1051/matecconf/20164605001.

[39] H. Häberlin, F. Volkenborn, M. Halfmann, and R. Haselhuhn, "Determination of fire safety risks at PV systems and development of risk minimization measures," in *Proc. 26th Eur. Photovoltaic Solar Energy Conf. Exhib.*, 2011, pp. 3553–3555, doi: 10.4229/26thEUPVSEC2011-4AV.2.23.

[40] Z. Zhang, J. Wu, L. Wang, F. Liu, P. Jia, L. Dai, Y. Lu, and T. Bian, "The analysis on simulation and invalidation of hot-spot temperature distribution in micro-defective crystalline silicon solar cells," *Renew. Energy*, vol. 147, pp. 2218–2228, Mar. 2020.

[41] Z. Wu, Z. Zhou, and M. Alkahtani, "Time-effective dust deposition analysis of PV modules based on finite element simulation for candidate site determination," *IEEE Access*, vol. 8, pp. 65137–65147, 2020, doi: 10.1109/ACCESS.2020.2985158.

[42] Z. Wu, W. Li, S. Kuka, and M. Alkahtani, "Analysis of dust deposition on PV arrays by CFD simulation," in *Proc. IECON-45th Annu. Conf. IEEE Ind. Electron. Soc.*, Lisbon, Portugal, Oct. 2019, pp. 5439–5443.

[43] N. G. Dhere and N. S. Shiradkar, "Fire hazard and other safety concerns of photovoltaic systems," *J. Photon. Energy*, vol. 2, no. 1, Dec. 2012, Art. no. 022006.

[44] F. Bayrak and H. F. Oztop, "Effects of static and dynamic shading on thermodynamic and electrical performance for photovoltaic panels," *Appl. Thermal Eng.*, vol. 169, Mar. 2020, Art. no. 114900.

[45] X. Ju, X. Zhou, J. Gong, K. Zhao, Y. Peng, C. Zhang, X. Ren, and L. Yang, "Impact of flat roof–integrated solar photovoltaic installation mode on building fire safety," *Fire Mater.*, vol. 43, no. 8, pp. 936–948, Dec. 2019, doi: 10.1002/fam.2755.

[46] P. Dunbabin, "Fire and solar PV systems—Recommendations for the fire and rescue services," Sci. Innov., Tech. Rep. P100874-1008, May 2017, no. 2.4.

[47] S. Silvestre, A. Boronat, and A. Chouder, "Study of bypass diodes configuration on PV modules," *Appl. Energy*, vol. 86, no. 9, pp. 1632–1640, Sep. 2009.

[48] K. A. Kim and P. T. Krein, "Reexamination of photovoltaic hot spotting to show inadequacy of the bypass diode," *IEEE J. Photovolt.*, vol. 5, no. 5, pp. 1435–1441, Sep. 2015, doi: 10.1109/JPHOTOV.2015.2444091.

[49] S. Daliento, F. D. Napoli, P. Guerriero, and V. D'Alessandro, "A modified bypass circuit for improved hot spot reliability of solar panels subject to partial shading," *Sol. Energy*, vol. 134, pp. 211–218, Sep. 2016.

[50] M. Dhimish, V. Holmes, P. Mather, and M. Sibley, "Novel hot spot mitigation technique to enhance photovoltaic solar panels output power performance," *Sol. Energy Mater. Sol. Cells*, vol. 179, pp. 72–79, Jun. 2018.

[51] P. Guerriero, P. Tricoli, and S. Daliento, "A bypass circuit for avoiding the hot spot in PV modules," *Sol. Energy*, vol. 181, pp. 430–438, Mar. 2019.

[52] M. Dhimish and G. Badran, "Current limiter circuit to avoid photovoltaic mismatch conditions including hot-spots and shading," *Renew. Energy*, vol. 145, pp. 2201–2216, Jan. 2020.

[53] *Outline of Investigation for Photovoltaic (PV) DC Arc-Fault Circuit Protection*, Underwriters Lab. Inc. (UL), Jan. 2013.

[54] G. Bao, X. Gao, R. Jiang, and K. Huang, "A novel differential high-frequency current transformer sensor for series arc fault detection," *Sensors*, vol. 19, no. 17, p. 3649, Aug. 2019.

[55] N. Gustavsson, "Evaluation and simulation of black-box arc models for high-voltage circuit breakers," Linköping Univ., Linköping, Sweden, Tech. Rep., Apr. 2004.

[56] X. Peng and J. Lai, "Application of clustering analysis on typical power consumption profile analysis," (in Chinese), *Power Syst. Protection Control*, vol. 19, pp. 68–73, Oct. 2014.

[57] C. Yao, P. Qiao, P. Chen, and Y. Chen, "Fractal antenna of 0.4 1 GHz for UHF monitoring of partial discharge in electrical equipment," *High Voltage Eng.*, vol. 40, pp. 2285–2291, Aug. 2014, doi: 10.13336/j.1003-6520.hve.2014.08.005.

[58] M. C. Damas and R. T. Robiscoe, "Detection of radio-frequency signals emitted by an arc discharge," *J. Appl. Phys.*, vol. 64, no. 2, pp. 566–574, Jul. 1988, doi: 10.1063/1.341971

[59] J. Johnson, S. Kuszmaul, W. Bower, and D. Schoenwald, "Using PV module and line frequency response data to create robust arc fault detectors," in *Proc. 26th Eur. Photovoltaic Sol. Energy Conf.*, 2011, pp. 3745–3750.

[60] J. Johnson, B. Pahl, C. Luebke, T. Pier, T. Miller, J. Strauch, S. Kuszmaul, and W. Bower, "Photovoltaic DC arc fault detector testing at Sandia National Laboratories," in *Proc. 37th IEEE Photovoltaic Spec. Conf.*, Jun. 2011, pp. 3614–3619.

[61] S. Chae, J. Park, and S. Oh, "Series DC arc fault detection algorithm for DC microgrids using relative magnitude comparison," *IEEE J. Emerg. Sel. Topics Power Electron.*, vol. 4, no. 4, pp. 1270–1278, Dec. 2016, doi: 10.1109/JESTPE.2016.2592186.

[62] B. Novak, "Implementing arc detection in solar applications: Achieving compliance with the new UL 1699B standard," Texas Instrum., Dallas, TX, USA, Corpus ID 30698940, 2012.

[63] S. Zhao, R. Zhang, and J. Du, "Photovoltaic series arc fault detection utilizing wavelet tranform," (in Chinese), *J. Huaqiao Univ.*, vol. 38, no. 1, Jan. 2017, doi: 10.11830/ISSN.1000-5013.201701002.

[64] H. Braun, S. T. Buddha, V. Krishnan, A. Spanias, C. Tepedelenlioglu, T. Yeider, and T. Takehara, "Signal processing for fault detection in photovoltaic arrays," in *Proc. IEEE Int. Conf. Acoust., Speech Signal Process. (ICASSP)*, Kyoto, Japan, Mar. 2012, pp. 1681–1684, doi: 10.1109/ICASSP.2012.6288220.

[65] S. Buddha, H. Braun, V. Krishnan, C. Tepedelenlioglu, A. Spanias, T. Yeider, and T. Takehara, "Signal processing for photovoltaic applications," in *Proc. IEEE Int. Conf. Emerg. Signal Process. Appl.*, Las Vegas, NV, USA, Jan. 2012, pp. 115–118, doi: 10.1109/ESPA.2012.6152459.

[66] F. Schimpf and L. E. Norum, "Recognition of electric arcing in the DC-wiring of photovoltaic systems," in *Proc. INTELEC-31st Int. Telecommun. Energy Conf.*, Incheon, South Korea, Oct. 2009, pp. 1–6, doi: 10.1109/INTLEC.2009.5352037.

[67] X. Yao, L. Herrera, S. Ji, K. Zou, and J. Wang, "Characteristic study and time-domain discrete- wavelet-transform based hybrid detection of series DC arc faults," *IEEE Trans. Power Electron.*, vol. 29, no. 6, pp. 3103–3115, Jun. 2014, doi: 10.1109/TPEL.2013.2273292.

[68] H. Zhu, Z. Wang, and R. S. Balog, "Real time arc fault detection in PV systems using wavelet decomposition," in *Proc. IEEE 43rd Photovoltaic Spec. Conf. (PVSC)*, Portland, OR, USA, Jun. 2016, pp. 1761–1766, doi: 10.1109/PVSC.2016.7749926.

[69] Z. Wang and R. S. Balog, "Arc fault and flash signal analysis in DC distribution systems using wavelet transformation," *IEEE Trans. Smart Grid*, vol. 6, no. 4, pp. 1955–1963, Jul. 2015.

[70] H. Lan and R. Zhang, "Study on the feature extraction of fault arc sound signal based on wavelet analysis," *Proc. CSU-EPSA*, vol. 20, no. 4, pp. 57–62, 2008.

[71] M. Rabla, E. Tisserand, P. Schweitzer, and J. Lezama, "Arc fault analysis and localisation by cross-correlation in 270 V DC," in *Proc. IEEE 59th Holm Conf. Electr. Contacts (Holm)*. Newport, RI, USA: IEEE, Sep. 2013, pp. 1–6.

[72] C. Wu, W. Xu, Z. Li, and L. Xu, "Arc fault type identification and circuit protection in photovoltaic system," (in Chinese), in *Proc. CSEE*, vol. 37, Mar. 2017, doi: 10.13334/j.0258-8013.pcsee.161894.

[73] Q. Lu, T. Wang, B. He, T. Ru, and D. Chen, "A new series arc fault identification method based on wavelet transform," in *Proc. IECON-43rd Annu. Conf. IEEE Ind. Electron. Soc.*, Oct. 2017, pp. 4817–4822.

[74] C. Wu, Y. Hu, Z. Li, and W. Fei, "On-line detection and location of DC bus arc faults in PV systems based on SSTDR," (in Chinese), in *Proc. CSEE*, Mar. 2020, doi: 10.13334/j.0258-8013.pcsee.191757.

[75] G. Yunmei, W. Li, W. Zhuoqi, and J. Binfeng, "Wavelet packet analysis applied in detection of low-voltage DC arc fault," in *Proc. 4th IEEE Conf. Ind. Electron. Appl.*, May 2009, pp. 4013–4016.

[76] C. Luebke, T. Pier, B. Pahl, D. Breig, and J. Zuercher, "Field test results of DC arc fault detection on residential and utility scale PV arrays," in *Proc. 37th IEEE Photovoltaic Specialists Conf.*, Seattle, WA, USA, Jun. 2011, pp. 001832–001836.

[77] C. Wu, X. Feng, T. Yuan, Z. Li, and Y. Zhong, "Photovoltaic arc fault detection method based on BP neural network," *Acta Energiae Solaris Sinica*, vol. 11, no. 37, pp. 2958–2964, 2016.

[78] Y. He, Q. Xu, S. Yang, and B. Yu, "A power load probability density forecasting method based on RBF neural network Quantile regression," (in Chinese), *Proc. CSEE*, vol. 33, no. 1, pp. 93–98, 2013.

[79] X. Ding, H. Zhu, H. Yin, and Y. Wang, "DC arc fault detection based on machine learning method," (in Chinese), *Transducer Microsyst. Technol.*, vol. 36, no. 7, pp. 123–127, 2017.

[80] J. A. Momoh and R. Button, "Design and analysis of aerospace DC arcing faults using fast Fourier transformation and artificial neural network," in *Proc. IEEE Power Eng. Soc. Gen. Meeting*, Jul. 2003, pp. 93–788.

[81] X. Lu, P. Lin, S. Cheng, Y. Lin, Z. Chen, L. Wu, and Q. Zheng, "Fault diagnosis for photovoltaic array based on convolutional neural network and electrical time series graph," *Energy Convers. Manage.*, vol. 196, pp. 950–965, Sep. 2019.

[82] G. Zhang, *Intelligent Control System and Application*, (in Chinese). Beijing, China: China Electric Power Press, 2007.

[83] Z. Wang and R. S. Balog, "Arc fault and flash detection in photovoltaic systems using wavelet transform and support vector machines," in *Proc. IEEE 43rd Photovoltaic Spec. Conf. (PVSC)*, Jun. 2016, pp. 3275–3280.

[84] K. Yang, R. Zhang, J. Yang, C. Liu, S. Chen, and F. Zhang, "A novel arc fault detector for early detection of electrical fires," *Sensor*, vol. 16, no. 4, pp. 1–24, 2016.

[85] B. Grichting, J. Goette, and M. Jacomet, "Cascaded fuzzy logic based arc fault detection in photovoltaic applications," in *Proc. Int. Conf. Clean Electr. Power (ICCEP)*, Taormina, Italy, Jun. 2015, pp. 178–183, doi: 10.1109/ICCEP.2015.7177620.

[86] M. Dhimish, V. Holmes, B. Mehrdadi, M. Dales, and P. Mather, "Photovoltaic fault detection algorithm based on theoretical curves modelling and fuzzy classification system," *Energy*, vol. 140, pp. 276–290, Dec. 2017.

[87] S. Martin, "Fire safety and solar electric and photovoltaic systems," *Fire*, vol. 107, no. 1363, 2013, p. 33.


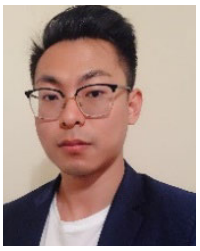

**ZUYU WU** was born in Shaanxi, China, in December 05, 1990. He received the B.Eng. and M.Eng. degrees in electrical engineering from Newcastle University, Newcastle, U.K., in 2011 and 2015, respectively. He is currently pursuing the Ph.D. degree with the University of York. His research interests include photovoltaic soiling management and the MPPT of PV power generation.

**YIHUA HU** (Senior Member, IEEE) received the B.S. degree in electrical motor drives and the Ph.D. degree in power electronics and drives from the China University of Mining and Technology, in 2003 and 2011, respectively. From 2011 to 2013, he was a Postdoctoral Fellow of the College of Electrical Engineering, Zhejiang University. From 2013 to 2015, he worked as a Research Associate at the Power Electronics and Motor Drive Group, University of Strathclyde. He is currently a Lecturer with the Department of Electrical Engineering and Electronics, University of York. He has published 65 articles in the IEEE TRANSACTIONS journals. His research interests include renewable generation, power electronics converters and control, electric vehicles, more electric ship/aircraft, smart energy systems, and non-destructive test technology. He is an Associate Editor of *IET Renewable Power Generation*, *IET Intelligent Transport Systems*, and *Power Electronics and Drives*.

**JENNIFER X. WEN** was born in Sichuan, China. She studied mechanical engineering at Shanghai Jiao Tong University, from 1980 to 1984. Upon graduation, she won one of the only three fully-funded scholarships among more than 200 graduates in her department for study abroad. This has supported her to conduct Ph.D. degree research on condensation heat transfer at Queen Mary College, University of London, from 1985 to 1988. Her professional career started in 1988, firstly with Computational Dynamics Ltd., now CD-Adapco, where she worked on the development of STAR-CD, a general-purpose computational fluid dynamics (CFD) code. She left CD-Adapco to join the Watson House Research Centre of the former British Gas plc, in 1991, working on the numerical study of multi-dimensional laminar flames with detailed chemistry. She returned to academia, in 1993, initially with London South Bank University and moved to Kingston University, as a Reader, in 1998, and was awarded the Professorial title after 18 months. She established and led the World-Class Centre for Fire and Explosion Studies at Kingston University for over ten years. She was also the Director of research for the former School of Engineering and then the Faculty of Engineering at Kingston University for over ten years.

**FUBAO ZHOU** was born in Nanjing, China, in July 1976. He received the Ph.D. degree in engineering from the China University of Mining and Technology, in June 2003.

Since 2011, he has been the Deputy Director of the Internet of Things (Perceived Mine) Research Center, China University of Mining and Technology, the Executive Dean of the School of Safety Engineering, the Dean of the School of Safety Engineering, and the Director of the Office of Talent Work. In April 2019, he became a member of the Standing Committee and the Vice President of the Party Committee of the China University of Mining and Technology. He is mainly engaged in mine disaster prevention and the utilization of resources, occupational health, and public safety research. He presided over more than 30 scientific research projects such as the 13th Five-Year Plan Key Research and Development Program, the National 111 Program Innovation and Intelligence Base, the National Science Foundation for Distinguished Young People, the National Natural Science Foundation's Key (Coal Joint) Project, and the Ministry of Education's Innovation Team Development Plan. He achieved the second prize of national scientific and technological achievements, and the first prize of the provincial and ministerial scientific and technological progress. He holds more than 30 patents for authorized national inventions and four pieces of software copyright, and has authored one academic monograph. He had been the editor-in-chief of two teaching materials.

**XIANMING YE** received the B.Eng. and M.Eng. degrees from the Department of Automation, Wuhan University, China, in 2008 and 2010, respectively, and the Ph.D. degree in electrical engineering from the University of Pretoria, in 2015. He conducted research on the design of optimal measurement and verification strategies for the national energy efficiency and demand-side management program at the Center of New Energy Systems, University of Pretoria. He is currently a Senior Lecturer with the Department of Electrical, Electronics, and Computer Engineering, University of Pretoria, South Africa. He is also a Certified Measurement and Verification Professional. His research interests include energy efficiency and demand-side management, building and industrial energy system modeling and optimization, renewable energy, microgrids, P2P energy sharing, battery management systems, and electric vehicles. He is currently a Guest Editor of IEEE ACCESS and an Associate Editor of the *IET Renewable Power Generation* journal.